

Impact of Copper Oxide Nanoparticles on Adult Rat Ovary and Possible Protective Effect of Selenium: A Histological and Immunohistochemical Study

Abeer Mohamed Ali Shalaby^{1*}, Eman Shaaban Abdel-Aziz Abul-Ela¹,
Amal Mohamed Moustafa¹, Shehab Hafez Mohamed¹

¹Medical Histology and Cell Biology Department, Faculty of Medicine, Mansoura University,
35516, Egypt

Corresponding author: Abeer Mohamed Ali Shalaby

E-mail: abeer_shalaby_777@mans.edu.eg

Abstract:

Copper oxide nanoparticles are thought to be an important transition metal oxide due to their interesting properties. Selenium is an important structural component of numerous enzymes, including glutathione peroxidase (GPx), thioredoxin reductase, as well as deiodinases. The present work was undertaken to evaluate the histological and immunohistochemical alterations in the adult rat ovary after oral administration of CuO-NPs, and to assess the potential ameliorative impact of selenium. Sixty adult female albino rats were equally divided in two major groups: group I and group II. Group I was further divided into three groups: control group IA, group IB: given 2000 mg/kg CuO-NPs once, group IC: received selenium (0.5 mg/kg), five days before giving one high dose of 2000 mg/kg CuO-NPs. Thereafter, given selenium for 14 days. group II was subdivided into three groups: group IIA (control), group IIB: received 300 mg/kg/day of CuO-NPs for 28 days, group IIC: received selenium (0.5 mg/kg), five days before starting concomitant administration of 300 mg/kg CuO-NPs and 0.5 mg/kg selenium for 28 days. Both group IB and group IIB showed signs of follicle and corpora lutea degeneration and revealed increased numbers of apoptotic bodies and atretic follicles. Increased reactions for caspase 3 and decreased reactions for BCL2 were also demonstrated. Apoptosis was greater in group IB. Group IC and group IIC showed apparent improvement of the histological structure, decreased numbers of apoptotic bodies (by 34.3% for the acute study and 38% for the chronic study), decreased atretic follicles (by 37.5% for the acute study and 34.78% for the chronic study), decreased reactions for caspase 3 and increased reactions for BCL2 as compared to groups IB and IIB respectively.

Conclusion: Selenium could reduce the damage induced by CuO-NPs in adult rat ovaries.

Key words: Copper Oxide Nanoparticles, Selenium, Ovary, Caspase 3, BCL2.

1. Introduction:

Nanomaterial is the material that has one or more external dimensions in the nanoscale. Metal nanoparticles received great attention because they had many applications in agriculture and the biomedical field.^[1] CuO-NPs have been employed in batteries, utilized as catalysts, and were included in gas sensors as well as high temperature superconductors. Additionally, copper oxide is known for its effective antibacterial properties. However, several investigations show that CuO-NPs are more harmful than other accessible metal oxide nanoparticles.^[2] Copper oxide nanoparticles could be released to the environment at various points in a product's life cycle such as production, transportation, usage, and removal. They are discharged into the environment through either deliberate or accidental means.^[3] Intentional release involves using CuO-NPs to remediate contaminated soils and groundwater as an antibacterial agent, as well as using CuO-NPs as an

adsorbent to eliminate arsenic from drinking water.^[4]Copper oxide nanoparticles were considered efficient adsorbent materials because of their small dimensions, large surface area, availability of raw materials for production and cost-effective manufacturing process.^[5]Unintentional discharge involves air, solid waste, and wastewater from production facilities. Copper oxide nanoparticles can migrate long distances to aquatic systems through wastewater effluents, direct discharges, or accidental spillages. Furthermore, CuO-NPs can be transported by wind or rainwater runoff, leading to their redistribution in the environment.^[6]Moreover, the presence of CuO-NPs in food packaging was previously reported.^[7]Nanoparticles (NPs) mainly enter the body by being inhaled, ingested, or absorbed through the skin and bloodstream. Upon entering the body, they are carried by the bloodstream to various body organs.^[8]Previous reports have revealed the harm caused by CuO-NPs in different organs including brain^[9], skin^[10], lungs^[11], male reproductive organs^[12], liver^[13], blood cells^[14], and kidneys^[15]. However, there is lack of studies regarding the histological alterations in ovarian tissue after exposure to CuO-NPs. Cells of the female reproductive organs were reported to gather nanoparticles through mechanisms that are not yet fully understood, which increases reactive oxygen species (ROS) levels. Their accumulation in the somatic cells of the ovary greatly hindered the oocyte's developmental ability.^[7]

Selenium is an important micronutrient that can be found naturally either in organic or inorganic states. Selenium is involved in multiple biochemical processes that are important to human health.^[16] It is critical building block of numerous enzymes. These enzymes are essential for antioxidation, reproduction, muscular function, and tumor prevention.^[17] Studies conducted on adult ovaries showed that selenium might have had a regulatory effect on maturation of granulosa cells and secretion of 17 β -estradiol.^[18] Moreover, large healthy follicles showed high levels of selenium and selenoproteins which might be a strong antioxidant during growth and the proliferation of follicles.^[19]

This work was undertaken to investigate histological as well as immunohistochemical alterations in adult rat ovaries associated with oral administration of CuO-NPs. The possible ameliorative influence of selenium, histologically and immunohistochemically, was also assessed.

2. Material and Methods:

Chemicals:

- 1- Copper oxide nanoparticles were bought from SIGMA company (No: 544868).
- 2- Sodium selenite 99% powder was purchased from SIGMA company (No: 214485).

Experimental animals and protocol

The protocol was given the approval of the IRB, Mansoura university (MDP.20.03.38). Sixty adult female albino rats, three months old, ranging in weight from 150-200 gm, were utilized in the present research. The animals were housed individually in cages at a temperature of 20°C, exposed to twelve-hour cycles of light and darkness, and were provided with unlimited nourishment and hydration.

Animal grouping:

Animals were equally separated into two major groups:

Group I (acute oral toxicity): Rats further evenly separated into three groups (10 animals in each group):

Group IA (control for acute oral toxicity): The animals were divided into two equal subgroups (each including 5 rats):

Group IA (1): received distilled water five days before starting the experiment, that was continued daily through the experiment for fourteen days.

Group IA (2): given only selenium, at a concentration of 0.5 mg/kg, five days before starting the experiment, that was continued daily through the experiment for fourteen days.

The dosing of selenium (0.5 mg/kg) was done by dissolving sodium selenite powder in distilled water.^[20,21] The calculated doses were individually prepared before the administration for each rat.

Group IB (acute CuO-NPs group): rats received one high dose of CuO-NPs at a concentration of 2000 mg/kg orally by gavage and were observed for fourteen days.

The administration of nanoparticles was conducted by suspending them in distilled water. The doses were prepared individually for each rat before being administered. The acute dose suspensions were created at a dosage of 200 mg/ml of distilled water. The rats received the suspensions orally through gavage in a volume of 1 ml per 100 grams of body weight (i.e., the acute dose; 2000 mg/kg).^[22]

Group IC (acute CuO-NPs + selenium): rats were given selenium via oral gavage (0.5 mg/kg), five days before administering one high oral dose of 2000 mg/kg CuO-NPs. Thereafter, selenium was administered every day for fourteen days.

Group II (chronic oral toxicity):

Animals further evenly separated into three groups (10 animals in each group):

Group IIA (control for chronic toxicity): Animals were divided into two equal subgroups (each including 5 rats):

Group IIA (1): received distilled water five days before starting the experiment, that was continued daily through the experiment for twenty-eight days.

Group IIA (2): given only selenium, at a concentration of 0.5 mg/kg, five days before starting the experiment, that was continued daily through the experiment for twenty-eight days.

Group IIB (chronic CuO-NPs group): rats were given 300 mg/kg of CuO-NPs orally through gavage every day for twenty-eight days.

The concentration of the chronic dose suspensions was 30 mg/ml of distilled water. The suspensions were given orally through gavage in a volume of 1 ml per 100 grams of body weight (i.e., the chronic dose; 300 mg/kg).^[22]

Group IIC (chronic CuO-NPs + selenium): rats were given selenium via oral gavage, in a dose of 0.5 mg/kg, five days before starting the experiment. Then, concomitant administration of CuO-NPs (300 mg/kg) and selenium (0.5 mg/kg), daily, orally, for twenty-eight days.

Obtaining the specimens

When the observation period ended (after a 14-day acute study and a 28-day chronic study), the animals were prepared for obtaining the samples. Vaginal smears were obtained and examined daily for the next 4 consecutive days. Animals were sacrificed only in the preovulatory day (proestrus phase). This phase was demonstrated by predominance of nucleated epithelial cells, that were present either individually or in clumps, and presence of few non nucleated cornified epithelial cells (**Fig.1**). The ovaries were immediately put in a 10% formalin buffer, and subsequently prepared for paraffin sectioning for examination under the light microscope.

Method of vaginal lavage:

A little quantity of distilled water was introduced into the vaginal canal by a non-invasive method using a sterile latex bulb. The latex bulb containing 100µl of distilled water was put at the beginning of the vagina, gently squeezed, and distilled water was pushed into the vaginal canal. The pressure gradually decreased, causing the water to be sucked back into the tip. The process was carried out 4-5 times before the liquid was put onto a glass slide, left to dry in air, stained with crystal violet, then inspected using the light microscope.^[23]

0.1% crystal violet stain was made by mixing 100 ml of distilled water with 0.1 gm of crystal violet powder. The dry slides were immersed in a jar with crystal violet stain for one minute. Then, the slides were removed to a second jar containing distilled water. Distilled water was used to rinse the slides for 60 seconds. The steps were repeated.^[24]

Preparation of tissue samples

Light Microscopic Study

Specimens from the ovaries were kept in a 10% neutral formalin buffer and treated according to the regular protocol to produce paraffin blocks. Serial sections measuring five micrometers in thickness were sliced and stained by H&E for conventional histopathological evaluation.^[25]

Methodology of immunohistochemical staining of caspase 3 and BCL2:

Some sections underwent immunohistochemical staining to demonstrate caspase 3 and BCL2 immunoreactions (markers for apoptosis).^[26]

The deparaffinized paraffin sections (5 micrometers) were used on coated slides for immunohistochemical analysis to locate caspase 3 and BCL2 through use of ABCImmune-peroxidase method.

The slides were:

- left in H₂O₂ for ten minutes to inhibit the natural peroxidase.
- rinsed in PBS for another ten minutes.
- Immersed in citrate buffer with a pH of 6, then heated in a microwave at 100°C for ten minutes to uncover antigenic peptides (Antigen retrieval).
- Incubated with primary antibodies of caspase 3 (1:1000 dilution)^[27], and BCL2 (1:100)^[28] overnight at 4°C.
 - ❖ Anti-caspase 3 was a rabbit polyclonal antibody, IgG₁ (catalogue No: ab4051, Abcam, UK).
 - ❖ Anti-BCL2 was a rabbit polyclonal antibody, IgG (catalogue No: ab59348, Abcam, UK).
- The primary antibodies were detected by adding two droplets of secondary antibody labeled with biotin.
 - ❖ Secondary antibody was anti-rabbit labeled with biotin (1:200, PK-4001; Chinese Fir Golden Bridge Company)
- Next, the slides were kept at room temperature for ten minutes in a solution of 1/200 concentration of bovine serum albumin dissolved in phosphate buffered saline to avoid any non-specific background staining.
- Incubating with DAB (Diaminobenzidine) substrate chromogen for five to ten minutes produced a brown precipitate being formed at the reaction site.
- Counterstaining using Mayer's Hematoxylin was done.^[29]

Procedures for ensuring the quality of immunostaining techniques:

Tissue sections containing samples from positive tissue controls (tonsil for caspase 3^[30] and lymph node for BCL2^[31]) were used to assess the effectiveness of the reagents (**Figs. 2A & B**).

Sections from the control ovaries without primary antibodies were added to tissue sections as well. Evaluating the background staining is crucial by examining these negative control sections. The lack of cross reactivity with primary antibodies is confirmed by the absence of specific staining in these slides (**Fig. 2C**).

Morphometric study and statistical analysis

- The number of apoptotic bodies / HPF (high-powered field x 400) and the number of atretic follicles / IPF (intermediate-powered field x 100) were counted in H & E sections. The positive caspase 3 and BCL2 reactions were quantified as a percentage per high-powered field (x 400). Six slides were analyzed for each animal in the study. Morphometric data for apoptotic bodies, caspase 3 and BCL2 was estimated by randomly selecting ten non-overlapping HPF (x 400). Morphometric data for atretic follicles was estimated by randomly selecting five non-overlapping IPF (x 100). The images obtained were assessed using video test morphology® software on a computer with Intel® Core I3® processor (Russia).
- The morphometric information was input, organized, and assessed with the software SPSS version 26.0 to generate the mean and SD.
- ANOVA was employed to make comparisons between numerical data from multiple groups.
- Further comparisons were obtained by applying post-hoc Tukey test.^[32]
- P value fewer than 0.05 was used as an indicator of a statistically significant result.

3. Results:

H&E Stain:

Control groups showed the same structure. Group IA (1) was used to represent all control groups. Sections of group IA (1) showed primordial follicles under the capsule of the ovary. Each primordial follicle consisted of an oocyte with a surrounding layer of flat follicular cells. Each multilaminar primary follicle consisted of an oocyte with surrounding multiple layers of cubical follicular cells. Each secondary follicle consisted of an oocyte that was encircled by zona pellucida and several layers of granulosa cells that were separated by an irregular cavity containing follicular fluid. The Graafian

follicle consisted of an oocyte that was encircled by zona pellucida and corona radiata. A fluid filled large follicular (antral) cavity separated the oocyte and its surroundings from multiple layers of granulosa cells. Granulosa and theca interna cells were separated by a basement membrane. Theca externa was seen outer to theca interna. Few apoptotic bodies were detected between the granulosa cells of mature follicles. The interstitial cells showed rounded nuclei and pale acidophilic cytoplasm (**Fig.3 A& B**). The corpus luteum was surrounded by a capsule of dense fibrous connective tissue. It was formed of granulosa lutein cells, which had rounded nuclei with prominent nucleoli, and theca lutein cells, which had smaller and darker nuclei. It also exhibited blood capillaries (**Fig.3 C**).

Group IB (acute CuO-NPs group) showed that some primordial follicles had degenerated oocytes, while some secondary follicles had vacuolated and degenerated oocytes and showed numerous apoptotic bodies between granulosa cells. The granulosa cell layers, and the antral cavity of mature follicles showed an apparent increase in apoptotic bodies in comparison with the control and the presence of spaces and necrotic debris. Some granulosa cells had elongated deeply stained nuclei (**Fig.4 A& B**). Some of the luteal cells had multiple intracytoplasmic vacuoles and pyknotic nuclei. Numerous apoptotic bodies and regular spaces were detected between luteal cells (**Fig.4 C**).

Group IC (acute CuO-NPs + selenium) showed no apparent degenerative changes in primordial and primary follicles. Vacuolations were detected within granulosa cells of some secondary follicles with fewer number of apoptotic bodies as compared to group IB. Some Graafian follicles showed oocytes with deep acidophilic vacuolated cytoplasm and separation of zona pellucida. Few apoptotic bodies were detected between granulosa cells, but there was no apparent spacing between the cells and no apparent necrotic debris (**Fig.4 D& E**). Corpora lutea exhibited fewer number of apoptotic bodies and fewer cells with intracytoplasmic vacuoles as compared to group IB (**Fig.4 F**).

Group IIB (chronic CuO-NPs group) showed that some primordial follicles were degenerated. The oocytes of some secondary follicles were irregular in shape and exhibited large vacuoles with separation of zona pellucida from the corona radiata. Numerous apoptotic bodies and cells with small, pyknotic nuclei were detected between granulosa cells. The oocytes of some Graafian follicles showed irregular nuclei and numerous small vacuoles in the cytoplasm. Features of apoptosis were detected in corona radiata, and many apoptotic bodies were seen in the cumulus oophorus and around the antral cavity. Spacing between granulosa cells was also detected (**Fig.5 A& B**). Corpora lutea were richly vascularized. Some granulosa lutein cells were necrotic and had degenerated nuclei. Apoptotic bodies were detected between luteal cells (**Fig.5 C**).

Group IIC (chronic CuO-NPs + selenium) showed that primordial and primary follicles had normal structures. Few apoptotic bodies were detected between granulosa cells of some secondary follicles. Separation of the zona pellucida from the oocyte, little spaces and fewer apoptotic bodies were detected between granulosa cells of some Graafian follicles of this group as compared to group IIB (**Fig.5 D& E**). Corpora lutea showed a normal structure (**Fig.5 F**).

Immune staining with anti-caspase 3:

Anti-caspase 3 stained control sections showed positive, brown-colored nuclear and cytoplasmic reactions in a few number of granulosa, interstitial, and luteal cells (**Fig.6 A& B**).

Group IB (acute CuO-NPs group) showed a relatively more intense positive immunoreaction for caspase 3 in nuclei and cytoplasm of granulosa and luteal cells as compared to control (**Fig.6 C& D**).

Group IC (acute CuO-NPs + selenium) showed a relatively less intense positive immunoreaction for caspase 3 in cytoplasm of granulosa and luteal cells as compared to group IB (**Fig.6 E& F**).

Group IIB (chronic CuO-NPs group) showed positive immunoreaction for caspase 3 in nuclei and cytoplasm of granulosa and luteal cells which was relatively more intense as compared to control group and relatively less intense as compared to group IB (**Fig.7 A& B**).

Group IIC (chronic CuO-NPs + selenium) showed positive immunoreaction for caspase 3 in nuclei and cytoplasm of granulosa, interstitial and luteal cells which was relatively less intense as compared to group IIB (**Fig.7 C& D**).

Immune staining with anti-BCL2:

Anti-BCL2 stained control sections showed brown positive reaction in the cytoplasm of granulosa, interstitial, and luteal cells (**Fig.8 A& B**).

Group IB (acute CuO-NPs group) showed less intense positive immunoreaction for BCL2 in granulosa and luteal cells' cytoplasm as compared to control. The interstitial cells showed a negative staining reaction (**Fig.8 C& D**).

Group IC (acute CuO-NPs + selenium) showed positive immunoreaction for BCL2 in granulosa and luteal cells' cytoplasm which was relatively more intense as compared to group IB. The cytoplasm of interstitial cells also showed positive immunoreaction (**Fig.8 E& F**).

Group IIB (chronic CuO-NPs group) showed negative immunoreaction for BCL2 in granulosa, interstitial and luteal cells' cytoplasm (**Fig.9 A& B**).

As compared to the negative reaction in Chronic CuO-NPs group, **group IIC (chronic CuO-NPs + selenium)** showed positive immunoreaction for BCL2 in granulosa, interstitial and luteal cells' cytoplasm (**Fig.9 C& D**).

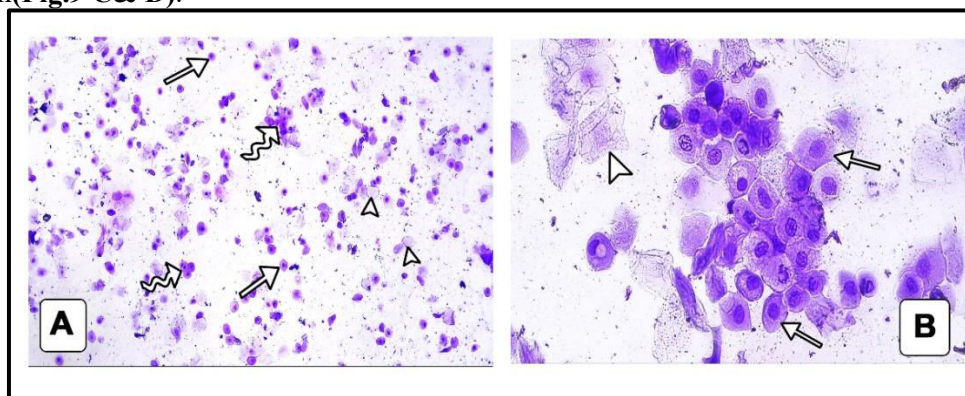


Figure (1): Cytological assessment of vaginal smears during proestrus phase. **A:** shows predominance of nucleated epithelial cells, that are present either individually (arrows) or in clumps (zigzag arrows). A few non nucleated cornified epithelial cells are also seen (arrowheads). **B:** A higher magnification of the nucleated epithelial cells (arrows) and the non-nucleated cornified epithelial cells (arrowhead) of a vaginal smear.

(Crystal violet stain: A × 100, B × 400)

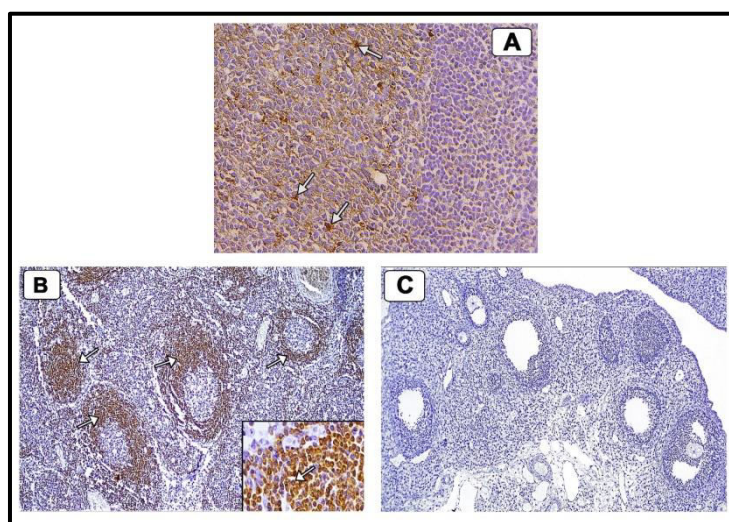


Figure (2): positive and negative tissue controls for immune stains. **A:** A photomicrograph of a paraffin section in the human tonsil. It shows brown positive immune reaction (arrows) in lymphocyte cytoplasm and is used as positive control for caspase 3. **B:** A section in rat lymph node. It shows brown positive immune reaction (arrows) and is used as positive control for Bcl-2. Inset: A higher magnification showing brown positive cytoplasmic immune reaction (arrow) for Bcl-2 in small non activated lymphocytes of the mantle zone. **C:** A section in control ovary after omitting the primary antibody (negative control) showing absence of the brown immune reaction.

(A:IHC for caspase3 \times 100,B:IHC for Bcl-2 \times 100. Inset \times 400 & C: IHC \times 100)

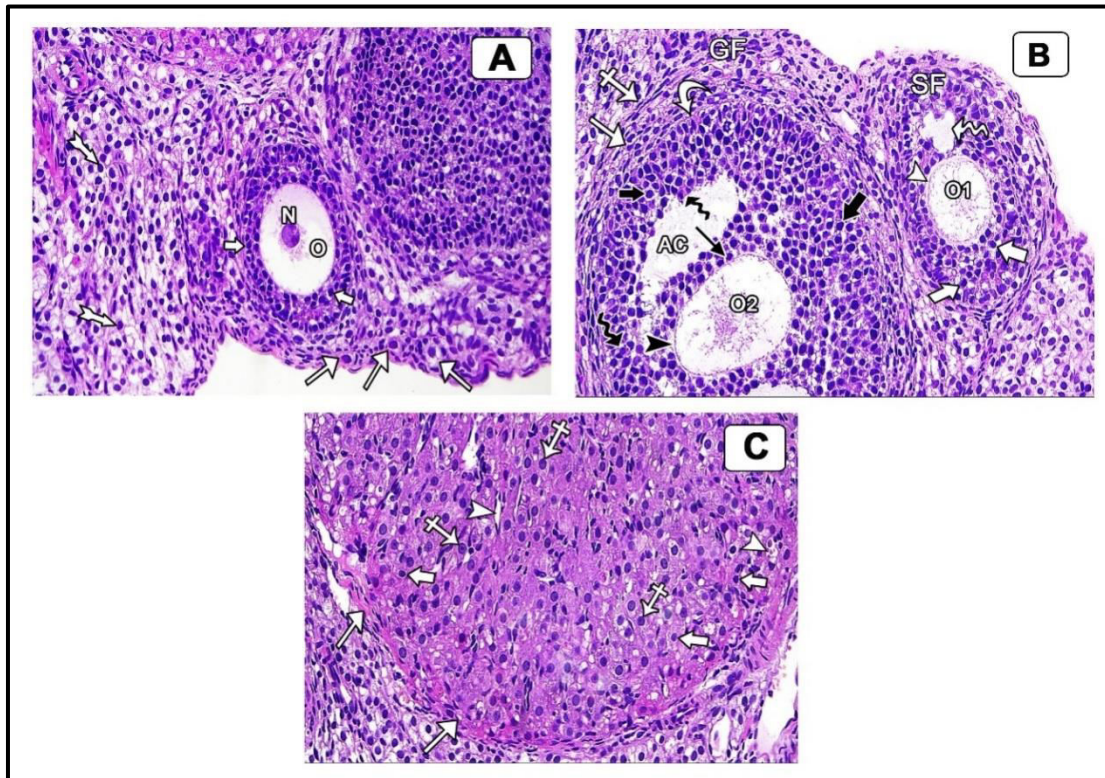


Figure (3): sections in control ovaries. **A:** shows a multilaminar primary follicle formed of an oocyte (O) with an open face nucleus (N) that is surrounded by multiple layers of cubical follicular cells (thick arrows). Primordial follicles (arrows) are seen under the ovarian surface. Each primordial follicle consists of an oocyte with a surrounding stratum of flat follicular cells. The interstitial cells (tailed arrows) show rounded nuclei and pale acidophilic cytoplasm. **B:** shows a secondary follicle (SF) and a Graafian follicle (GF). The secondary follicle consists of an oocyte (O1) that is encircled by zona pellucida (white arrowhead) and several layers of granulosa cells (white thick arrows). Between the granulosa cells, there is a small irregular cavity containing follicular fluid (white zigzag arrow). The Graafian follicle consists of an oocyte (O2) that is encircled by zona pellucida (black arrowhead) and corona radiata (black arrow). A single large antral cavity (AC) separates the oocyte and its surroundings from multiple layers of granulosa cells (black thick arrows). A basement membrane (curved arrow) separates granulosa cells from the theca interna (white arrow). Theca externa (crossed arrow) lies outer to theca interna. Few apoptotic bodies are noticed (black zigzag arrows). **C:** shows a part of a corpus luteum which is surrounded by a capsule of dense fibrous connective tissue (arrows). Granulosa lutein cells (crossed arrows) have rounded nuclei with prominent nucleoli. Theca lutein cells (thick arrows) have smaller and darker nuclei. Blood capillaries (arrowheads) are noticed.

(H&E \times 400)

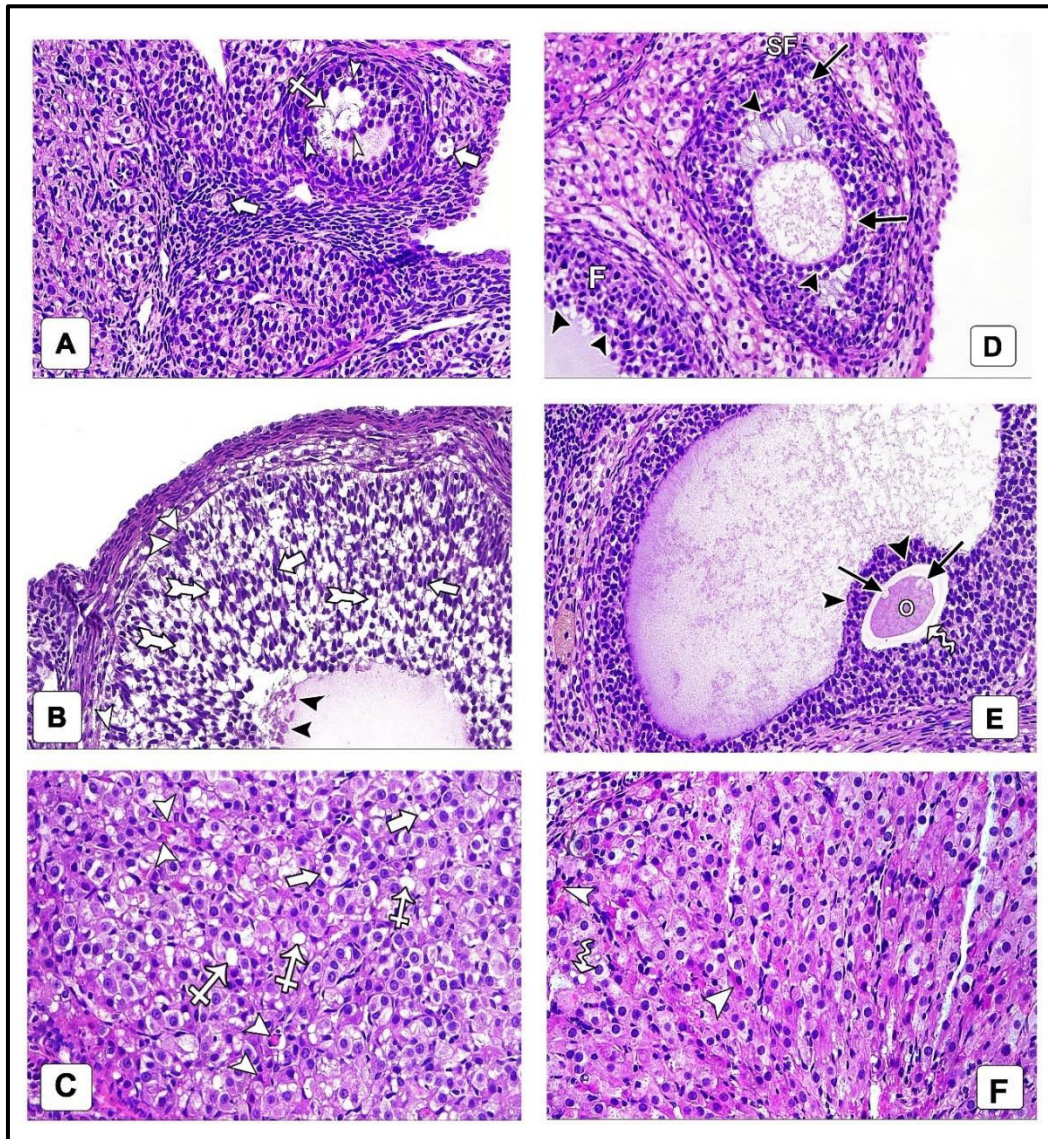


Figure (4): (A, B, C)sections from group IB.A: shows some primordial follicles with degenerated oocytes (thick arrows). A secondary follicle has a vacuolated and degenerated oocyte (crossed arrow) and shows numerous apoptotic bodies (arrowheads) between the granulosa cells. **B:** shows some granulosa cells with elongated deeply stained nuclei (thick arrows). Multiple spaces (tailed arrows) are seen between the granulosa cells. Apoptotic bodies (white arrowheads) and necrotic debris (black arrowheads) are noticed. **C:** shows that some luteal cells have multiple intracytoplasmic vacuoles with pyknotic nuclei (thick arrows). Many apoptotic bodies (arrowheads) and regular spaces (crossed arrows) are demonstrated between luteal cells. **(D, E, F)sections from group IC.** **D:** shows that granulosa cells of the secondary (SF) and mature follicle (F) have fewer number of apoptotic bodies (arrowheads) as compared to (A) and (B). Vacuolations (arrows) appear in granulosa cells of the secondary follicle. **E:** shows the oocyte of a mature follicle having a deep acidophilic cytoplasm (O) that contains vacuoles (arrows). The zona pellucida appears separated from the oocyte (zigzag arrow). Few apoptotic bodies (arrowheads) are demonstrated. **F:** shows fewer apoptotic bodies (arrowheads) and fewer granulosa lutein cells with intracytoplasmic vacuoles (zigzag arrow) as compared to (B).
(H&E x 400)

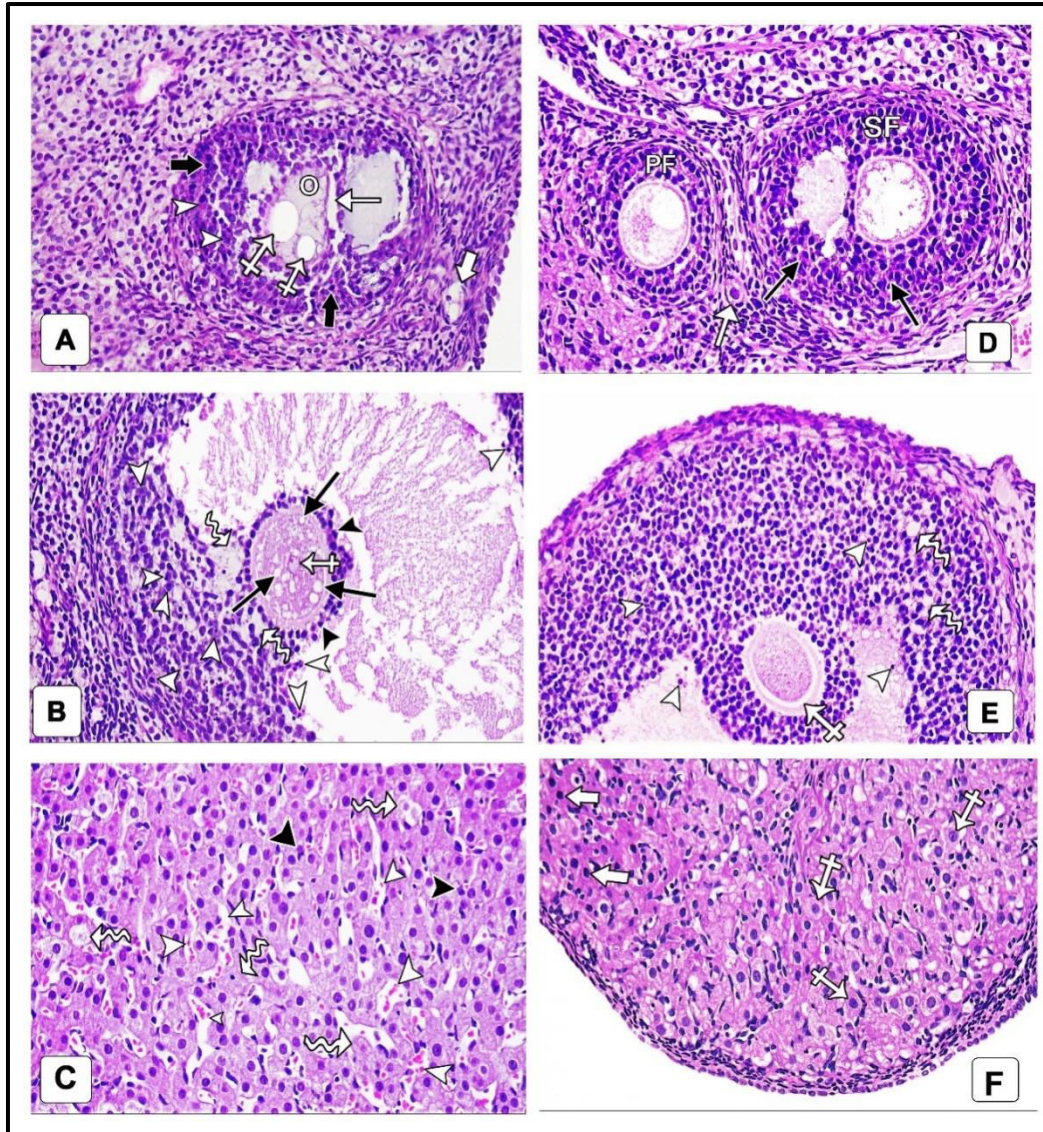


Figure (5): (A, B, C)sections from group IIB. A: shows a secondary follicle. The oocyte (O) appears irregular in shape and contains large vacuoles (crossed arrows). The zona pellucida is separated from the corona radiata by an irregular space (arrow). Granulosa cells show small and pyknotic nuclei (black thick arrows). Numerous apoptotic bodies (arrowheads) are demonstrated. A degenerated primordial follicle (white thick arrow) is noticed. **B:** shows a Graafian follicle. The oocyte shows an irregular nucleus (crossed arrow). Its cytoplasm contains numerous small vacuoles (arrows). Some cells of the corona radiata show features of apoptosis (black arrowheads). Many apoptotic bodies (white arrowheads) are noticed. Spacing between the cells of cumulus oophorus can also be noticed (zigzag arrows). **C:** shows that some granulosa lutein cells appear necrotic and show damaged nuclei (zigzag arrows). Apoptotic bodies (black arrowheads) are demonstrated. numerous blood capillaries (white arrowheads) are noticed. **(D, E, F)sections from group IIC. D:** shows normal primordial (white arrow), multilaminar primary (PF) and secondary (SF) follicles. Few apoptotic bodies (black arrows) are noticed between granulosa cells of the secondary follicle. **E:** shows a part of a Graafian follicle. Zona pellucida is separated from the oocyte (crossed arrow). As compared to (B), little spaces (zigzag arrows) and fewer apoptotic bodies (arrowheads) between granulosa cells are noticed. **F:** shows normal granulosa lutein (crossed arrows) and theca lutein (thick arrows) cells. (H&E x 400)

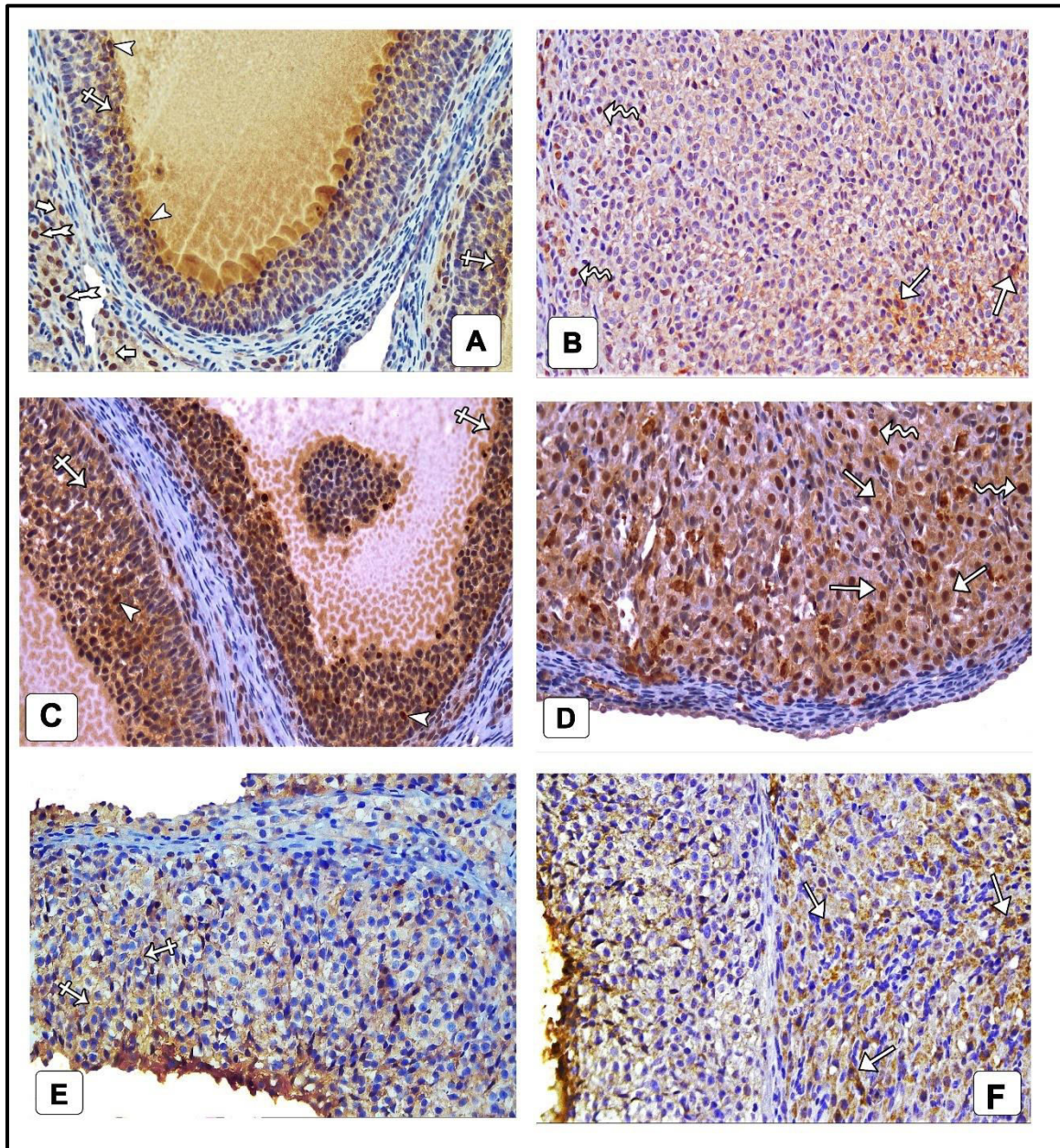


Figure (6): (A, B): sections from the control group. A: shows positive nuclear (arrowheads) and cytoplasmic (crossed arrows) immune reactions in a few number of granulosa cells. Nuclei (tailed arrows) and cytoplasm (thick arrows) of interstitial cells also show positive reactions. **B:** shows positive nuclear (zigzag arrows) and cytoplasmic (arrows) immune reactions in a few number of luteal cells. **(C, D): sections from group IB. C:** shows a relatively more intense positive nuclear (arrowheads) and cytoplasmic (crossed arrows) immune reactions in granulosa cells as compared to (A). **D:** shows a relatively more intense positive nuclear (arrowheads) and cytoplasmic (crossed arrows) immune reactions in luteal cells as compared to (B). **(E, F): sections from group IC. E:** shows a relatively less intense positive cytoplasmic (crossed arrows) immune reaction in granulosa cells as compared to (C). **F:** shows a relatively less intense positive cytoplasmic (arrows) immune reaction in luteal cells as compared to (D).
(IHC for caspase 3 ×400)

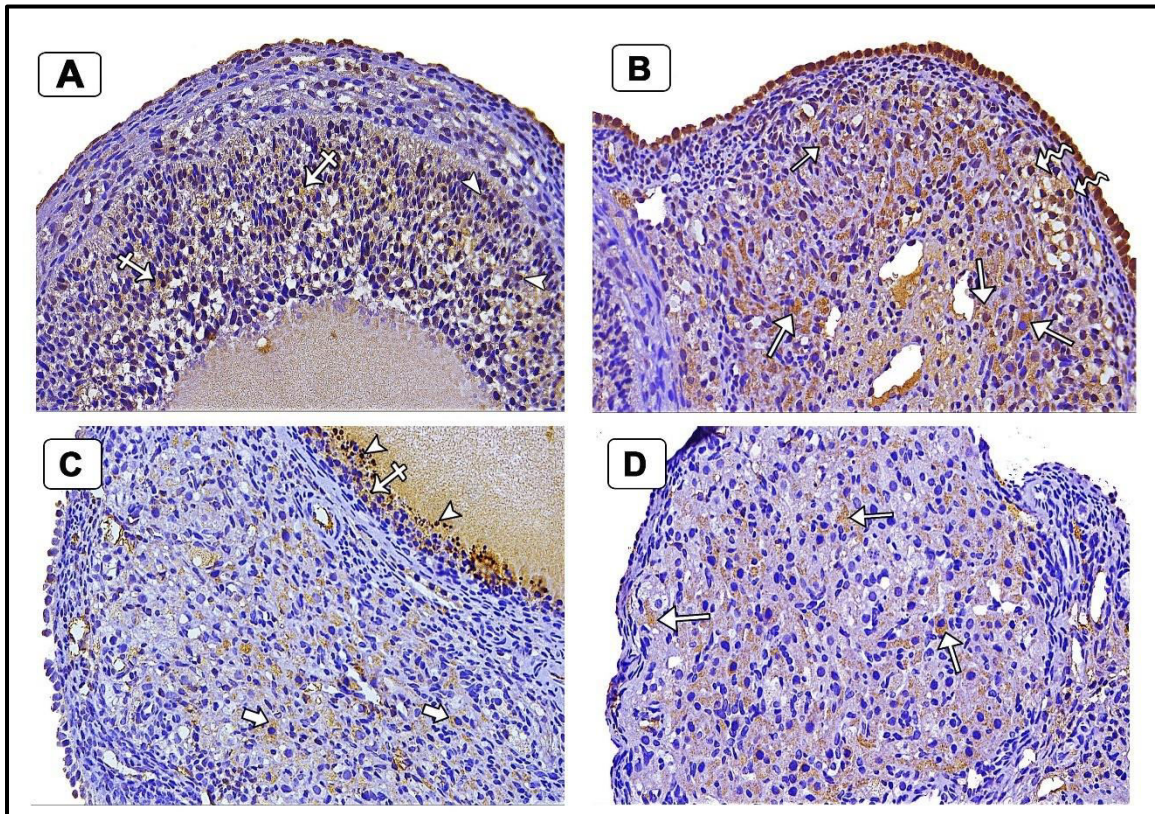


Figure (7): (A, B):sections from group IIB. A: shows positive nuclear (arrowheads) and cytoplasmic (crossed arrows) immune reactions in granulosa cells which are relatively more intense than control (Fig. 5A) and relatively less intense than group IB (Fig. 5C). **B:** shows positive nuclear (zigzag arrows) and cytoplasmic (arrows) immune reactions in luteal cells which are relatively more intense than control (Fig. 5B) and relatively less intense than group IB (Fig. 5D). **(C, D): sections from group IIC. C:** shows positive nuclear (arrowheads) and cytoplasmic (crossed arrows) immune reactions in granulosa cells which are relatively less intense as compared to (A). The cytoplasm of interstitial cells (thick arrows) also shows a positive immune reaction. **D:** shows positive cytoplasmic (arrows) immune reaction in luteal cells which is relatively less intense as compared to (B).
(IHC for caspase 3 ×400)

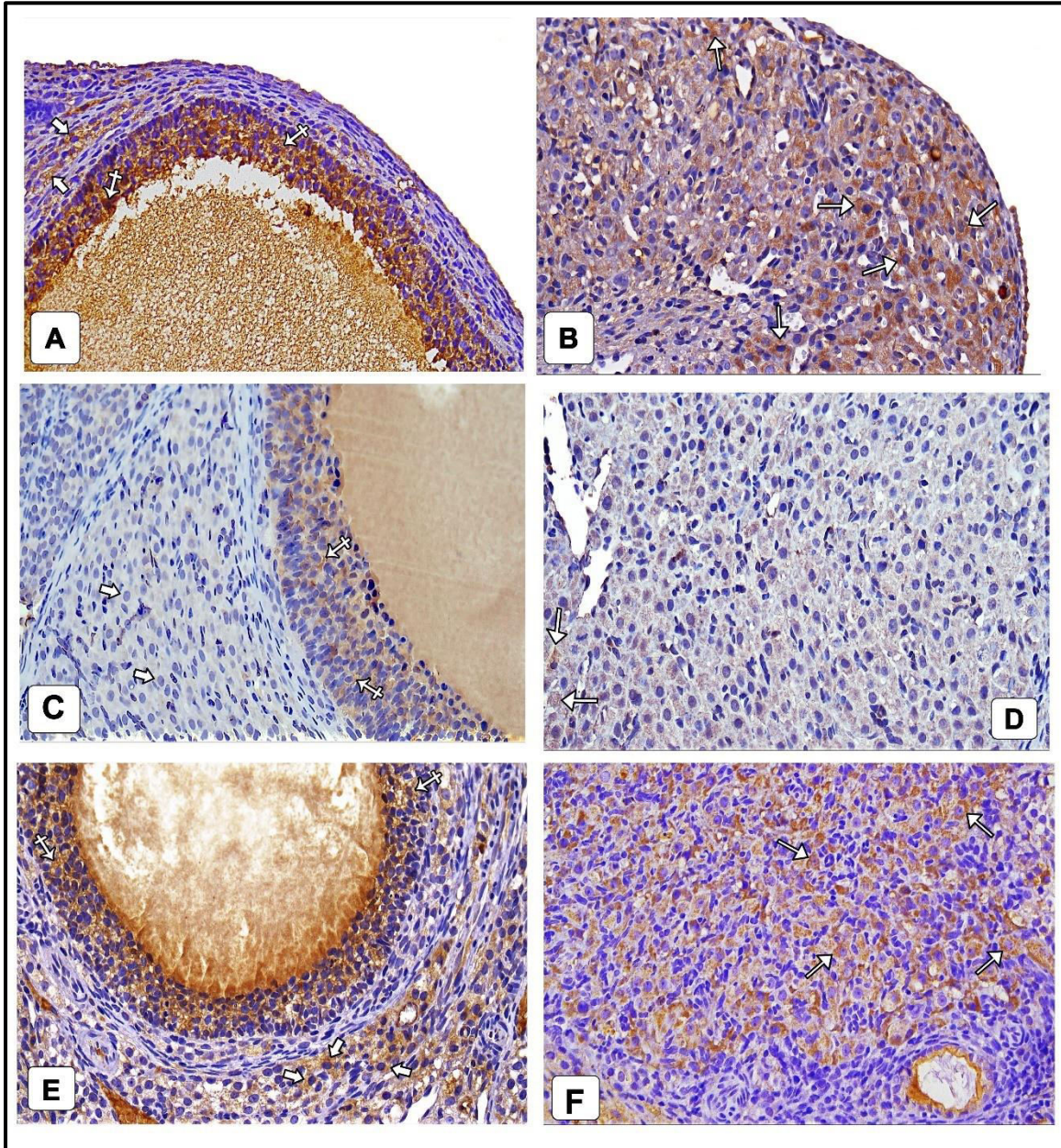


Figure (8): (A, B): sections from control ovaries. A: shows positive cytoplasmic immune reaction in granulosa cells (crossed arrows) and interstitial cells (thick arrows). **B:** shows positive cytoplasmic (arrows) immune reaction in luteal cells. **(C, D): sections from group IB. C:** shows a relatively less intense positive cytoplasmic (crossed arrows) immune reaction in granulosa cells as compared to (A). The interstitial cells (thick arrows) show negative immune reaction. **D:** shows a relatively less intense positive cytoplasmic (arrows) immune reaction in luteal cells as compared to (B). **(E, F): sections from group IC. E:** shows a relatively more intense positive cytoplasmic (crossed arrows) immune reaction in granulosa cells as compared to (C). A positive cytoplasmic (thick arrows) immune reaction is also detected in the interstitial cells. **F:** shows positive cytoplasmic (arrows) immune reaction in luteal cells which is relatively more intense as compared to (D).
(IHC for BCL2 ×400)

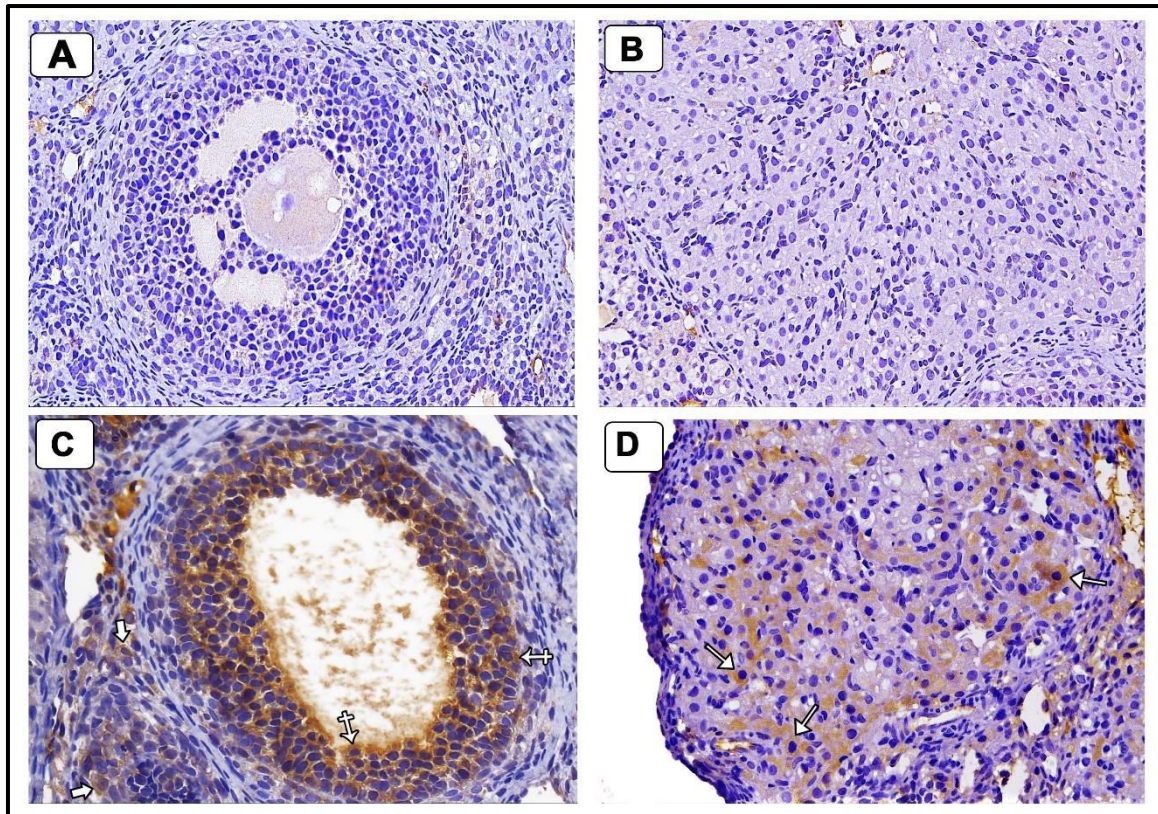


Figure (9): (A, B): sections from group IIB. A: shows negative immune reaction for BCL2 in granulosa cells, and in the interstitial cells. **B:** shows negative immune reaction for BCL2 in luteal cells. **(C, D): sections from group IIC. C:** shows positive cytoplasmic immune reaction in granulosa cells (crossed arrow) and in interstitial cells (thick arrows). **D:** shows positive cytoplasmic (arrows) immune reaction in luteal cells. (IHC for BCL2 $\times 400$)

Statistical analysis of morphometric results

Apoptotic bodies' count /HPF (high powered field):

Apoptotic bodies' count/HPF showed a significant rise ($P = <.001$) in group IB (67.9 ± 12.28) when compared to group IA (14.7 ± 3.2), while it was significantly decreased ($P = <.001$) in group IC (44.6 ± 9.14) when compared to group IB. So, selenium treatment in the acute study reduced the number of apoptotic bodies by approximately 34.3 %. Moreover, apoptotic bodies' count /HPF showed a significant rise ($P = <.001$) in group IIB (53.1 ± 8.5) when compared to group IIA (14.4 ± 3.57) and it showed a significant decrease ($P = 0.003$) when compared to group IB. Apoptotic bodies' count /HPF was also significantly decreased ($P = <.001$) in group IIC (32.9 ± 6.84) when compared to group IIB. So, combination of selenium with CuO-NPs in the chronic study reduced the number of apoptotic bodies by approximately 38 % (**Table 1**).

The number of atretic follicles/IPF (intermediate power field):

Atretic follicles' count /IPF showed a significant rise ($P = <.001$) in group IB (2.4 ± 0.52) when compared to group IA (1.2 ± 0.42), while it was significantly decreased ($P = 0.006$) in group IC (1.5 ± 0.53) when compared to group IB. So, selenium treatment in the acute study reduced the number of atretic follicles by approximately 37.5 %. Moreover, atretic follicles' count /IPF showed a significant rise ($P = <.001$) in group IIB (2.3 ± 0.82) when compared to group IIA (1.1 ± 0.32) and it was non-significantly changed ($P = 1$) when compared to group IB. Atretic follicles' count /IPF also showed a significant decrease ($P = 0.21$) in group IIC (1.5 ± 0.53) when compared to group IIB. So, combination of selenium with CuO-NPs in the chronic study reduced the number of atretic follicles by approximately 34.78 % (**Table 2**).

Caspase-3 percentage area:

Group IB showed a significant increase ($P = <.001$) in caspase-3 percentage area (60.57 ± 10.26) when compared to group IA (12.37 ± 1.6). Caspase-3 percentage area was significantly decreased ($P = <.001$) in group IC (27.31 ± 7.81) as compared to group IB. Moreover, caspase-3 percentage area was significantly increased ($P = <.001$) in group IIB (36.62 ± 9.05) when compared to group IIA (12.34 ± 3.6) and it was significantly lower ($P = 0.023$) when compared to group IB. Caspase-3 percentage area was also significantly decreased ($P = <.001$) in group IIC (25.54 ± 5.79) when compared to group IIB (Table 3).

BCL2 percentage area:

BCL2 percentage area was significantly decreased ($P = <.001$) in group IB (11.22 ± 3.56) when compared to group IA (50.3 ± 4.78), while it was significantly increased ($P = <.001$) in group IC (33.22 ± 3.62) when compared to group IB. Moreover, BCL2 percentage area was significantly decreased ($P = <.001$) in group IIB (15.26 ± 2.18) when compared to group IIA (51.79 ± 5.39) and it was non-significantly increased ($P = 0.433$) when compared to group IB. BCL2 percentage area was also significantly increased ($P = <.001$) in group IIC (38.63 ± 5.08) when compared to group IIB (Table 4).

Table (1): The number of apoptotic bodies (mean \pm SD) in control and experimental groups:

| | | Group IA (Control for acute toxicity) (n=10) | Group IIA (Control for chronic toxicity) (n=10) | Group IB (Acute CuO- NPs) (n=10) | Group IC (Acute CuO-NPs +Selenium) (n=10) | Group IIB (Chronic CuO-NPs) (n=10) | Group IIC (Chronic CuO-NPs +Selenium) (n=10) | ANOVA P Value |
|-------------|------------------|--------------------------------------------------------------|--------------------------------------------------------------------|--------------------------------------------------|-----------------------------------------------------------|-------------------------------------------------|--------------------------------------------------------------|------------------|
| NAB/ HPF | Mean \pm SD | 14.7 \pm 3.2 | 14.4 \pm 3.57 | 67.9 \pm 12.28 | 44.6 \pm 9.14 | 53.1 \pm 8.5 | 32.9 \pm 6.84 | |
| | P1 | | 1 | <.001* | <.001* | <.001* | <.001* | <.001* |
| | P2 | | | <.001* | <.001* | <.001* | <.001* | |
| | P3 | | | | <.001* | 0.001* | <.001* | |
| | P4 | | | | | 0.175 | 0.02* | |
| | P5 | | | | | | <.001* | |

SD: standard deviation. P: Probability. *: significance ≤ 0.05

Test used: One way ANOVA test followed by post-hoc Tukey.

P1: Significance relative to group IA (Control for acute toxicity).

P2: Significance relative to group IIA (Control for chronic toxicity).

P3: Significance relative to group IB (Acute cuo-nps).

P4: Significance relative to group IC (Acute cuo-nps + selenium).

P5: Significance relative to group IIB (Chronic cuo-nps).

NAB/HPF: number of apoptotic bodies/ high powered field.

Table (2): The number of atretic follicles (mean \pm SD) in control and experimental groups:

| | | Group IA (Control for acute toxicity) (n=10) | Group IIA (Control for chronic toxicity) (n=10) | Group IB (Acute CuO- NPs) (n=10) | Group IC (Acute CuO-NPs +Selenium) (n=10) | Group IIB (Chronic CuO-NPs) (n=10) | Group IIC (Chronic CuO-NPs +Selenium) (n=10) | ANOVA P Value |
|-------------|------------------|--------------------------------------------------------------|--------------------------------------------------------------------|--------------------------------------------------|-----------------------------------------------------------|-------------------------------------------------|--------------------------------------------------------------|------------------|
| NAF/ IPF | Mean \pm SD | 1.2 \pm 0.42 | 1.1 \pm 0.32 | 2.4 \pm 0.52 | 1.5 \pm 0.53 | 2.3 \pm 0.82 | 1.5 \pm 0.53 | |

| | | | | | | | | |
|--|-----------|--|--------------|------------------|---------------|------------------|---------------|------------------|
| | P1 | | 0.998 | <.001* | 0.819 | <.001* | 0.819 | <.001* |
| | P2 | | | <.001* | 0.574 | <.001* | 0.574 | |
| | P3 | | | | 0.006* | 0.998 | 0.006* | |
| | P4 | | | | | 0.021* | 1 | |
| | P5 | | | | | | 0.021* | |

SD: standard deviation. **P:** Probability. *****: significance ≤ 0.05

Test used: One way ANOVA test followed by post-hoc tukey.

P1: Significance relative to group IA (Control for acute toxicity).

P2: Significance relative to group IIA (Control for chronic toxicity).

P3: Significance relative to group IB (Acute CuO-NPs).

P4: Significance relative to group IC (Acute CuO-NPs + selenium).

P5: Significance relative to group IIB (Chronic CuO-NPs).

NAF/IPF: number of atretic follicles/ intermediate powered field.

Table (3): Percentage area of positive Caspase 3 immune reaction (mean \pm SD):

| | | Group IA (Control for acute toxicity) (n=10) | Group IIA (Control for chronic toxicity) (n=10) | Group IB (Acute CuO- NPs) (n=10) | Group IC (Acute CuO-NPs +Selenium) (n=10) | Group IIB (Chronic CuO-NPs) (n=10) | Group IIC (Chronic CuO-NPs +Selenium) (n=10) | ANOVA P Value |
|--------------------|------------------------------------|--------------------------------------------------------------------------|-------------------------------------------------------------------------------------|------------------------------------------------------------------|-----------------------------------------------------------------------|----------------------------------------------------------------|--------------------------------------------------------------------------|--------------------------|
| CPA (%) | Mean \pmSD | 12.37\pm 1.6 | 12.34\pm 3.6 | 60.57\pm 10.26 | 27.31\pm 7.81 | 36.62\pm 9.05 | 25.54\pm 5.79 | <.001* |
| | P1 | | 1 | <.001* | <.001* | <.001* | 0.001* | |
| | P2 | | | <.001* | <.001* | <.001* | 0.001* | |
| | P3 | | | | <.001* | <.001* | <.001* | |
| | P4 | | | | | 0.05* | 0.993 | |
| | P5 | | | | | | 0.011* | |

SD: standard deviation. **P:** Probability. *****: significance ≤ 0.05

Test used: One way ANOVA test followed by post-hoc tukey.

P1: Significance relative to group IA (Control for acute toxicity).

P2: Significance relative to group IIA (Control for chronic toxicity).

P3: Significance relative to group IB (Acute CuO-NPs).

P4: Significance relative to group IC (Acute CuO-NPs + selenium).

P5: Significance relative to group IIB (Chronic CuO-NPs).

CPA: Caspase 3 percentage area.

Table (4): percentage area of positive BCL2 immune reaction (mean \pm SD):

| | | Group IA (Control for acute toxicity) (n=10) | Group IIA (Control for chronic toxicity) (n=10) | Group IB (Acute CuO- NPs) (n=10) | Group IC (Acute CuO- NPs +Selenium) (n=10) | Group IIB (Chronic CuO-NPs) (n=10) | Group IIC (Chronic CuO-NPs +Selenium) (n=10) | ANOVA P Value |
|---------------------|------------------------------------|--------------------------------------------------------------------------|-------------------------------------------------------------------------------------|------------------------------------------------------------------|------------------------------------------------------------------------|------------------------------------------------------------|--------------------------------------------------------------------------|--------------------------|
| BCL2 (%) | Mean \pmSD | 50.3\pm 4.78 | 51.79\pm 5.39 | 11.22\pm 3.56 | 33.22\pm 3.62 | 15.26\pm 2.18 | 38.63\pm 5.08 | <.001* |
| | P1 | | 0.969 | <.001* | <.001* | <.001* | 0.001* | |
| | P2 | | | <.001* | <.001* | <.001* | 0.001* | |
| | P3 | | | | <.001* | 0.287 | <.001* | |
| | P4 | | | | | <.001* | 0.065 | |

| | | | | | | | |
|-----------|--|--|--|--|--|------------------|--|
| P5 | | | | | | <.001* | |
|-----------|--|--|--|--|--|------------------|--|

SD: standard deviation. **P:** Probability. *****: significance ≤ 0.05

Test used: One way ANOVA test followed by post-hoc tukey.

P1: Significance relative to group IA (Control for acute toxicity).

P2: Significance relative to group IIA (Control for chronic toxicity).

P3: Significance relative to group IB (Acute CuO-NPs).

P4: Significance relative to group IC (Acute CuO-NPs + selenium).

P5: Significance relative to group IIB (Chronic CuO-NPs).

4. Discussion

CuO-NPs were one of the initial nanoparticles produced. because of their unique features and important uses in different fields such as thermal and electrical devices as well as cosmetics.^[33] However, copper oxide nanoparticles were found to be the most powerful regarding cytotoxicity, DNA damage, and oxidative stress compared to other metal oxide particles, suggesting that exposure to them through occupation or consumer products could be harmful to health.^[34]

Selenium is a vital mineral that is required for regulating balance within the bodies of animals and humans. Selenium has a high antagonizing effect against oxidative stress and inflammation, besides its antibacterial properties.^[35]

In the current work, we examined the negative impacts of orally administered CuO-NPs on the ovaries of adult rats using histological and immunohistochemical findings as criteria. We also assessed the possibility of protection by selenium against the negative consequences of CuO-NPs on the ovary.

As food and water may contain nanoparticles, the choice was made to use the oral route for administration of CuO-NPs, because they could be consumed intentionally or accidentally.^[22] The dose of copper oxide nanoparticles that is fatal in Albino mice was reported to be 550 mg/kg body weight injected via venous route.^[36] Moreover, Elkhateeb et al^[37] mentioned that the CuO-NPs lethal dose exceeded 2500 mg/kg based on the MSDS from Sigma-Aldrich. Previously, Ouni et al^[38] gave rats CuO-NPs orally at levels of 250 and 500 mg/kg for two weeks to assess subacute toxicity and impacts on cognitive abilities. Bugata et al^[22] also investigated impacts of orally introduced copper oxide nanoparticles on female rats by giving one high dose “2000 mg/kg” and several lower doses “30, 300, and 1000 mg/kg” daily for four weeks to assess biochemical changes and oxidative stress markers in “liver, kidney, and brain”.

H&E-stained sections of CuO-NPs treated groups of this study (group IB and group IIB) revealed some degenerated primordial follicles’ oocytes and several degenerative changes in the oocytes of secondary and Graafian follicles. It was reported that CuO-NPs at concentrations exceeding one $\mu\text{g/ml}$ showed toxicity to the ovum and had deleterious effects on embryo development due to DNA damage. Oocytes developed in presence of one $\mu\text{g/ml}$ or less of copper oxide-NPs had reduced injury in comparison to others developed in absence of CuO-NPs. However, as the level of copper oxide-NPs was increased above one $\mu\text{g/ml}$, the level of DNA damage also increased, indicating that toxicity was triggered by higher CuO-NPs concentrations during oocyte maturation in vitro.^[39] Reports indicate that CuO-NPs either pass via a nuclear pore or cause physical injury to the nuclear membrane to interact with DNA within the nucleus. Binding of CuO to nuclear DNA activates two signaling pathways: MAPK and NF-kB. These pathways initiate inflammatory reactions and have been linked to cell death.^[40] Toxicity to oocytes has been observed with other metal oxide nanoparticles. In a previous study for the impact of nanoparticles of zinc oxide (ZnO NP) on cultured mouse oocytes, the findings indicated that ZnO nanoparticles resulted in meiotic abnormalities and death of mouse oocyte. They showed an adverse effect on oocyte development and survival in a manner that varied based on dosage and duration. Moreover, ZnO NP was found to enhance apoptosis and autophagy in the oocytes through the observed rise in caspase 3/7 activity.^[41]

On the contrary, group IC (acute CuO-NPs + selenium) revealed that most oocytes had a normal structure. However, some Graafian follicles showed oocytes with vacuolated cytoplasm. It was reported that selenium supplementation could potentially enhance follicle quality in polycystic ovary

syndrome patients with poor quality follicles caused by oxidative stress.^[42] Moreover, selenium supplementation enhanced yak oocyte maturation during in vitro maturation which was attributed to decreasing DNA damage and increasing total glutathione peroxidase activity in oocytes.^[43] Selenium was reported to have a modulatory effect on the activation of MAPK signaling pathway caused by BPA through reducing expression of ERK, JNK and p38.^[44]

Luteal cells of the acute toxicity rats (group IB) exhibited multiple intracytoplasmic vacuoles and pyknotic nuclei, while chronic toxicity rats (group IIB) showed larger spherical vacuoles in the cytoplasm of some luteal cells. Widely spaced large vacuoles in luteal cell, were described by Amelkina et al^[45] in domestic cats to depict autophagic vacuoles as a part of the processes involved in luteolysis. Signs of degeneration in corpus luteum were reported by Fatahian-Dehkordi, et al^[46] in mice treated with CuO-NPs. They stated that vacuolation in luteal cells may happen because of the inhibition of steroid production, resulting in the buildup of lipids in the cells. However, luteal cell vacuolation is commonly detected during the proestrus stage as part of corpus luteum degradation.^[47]

The H&E-stained control sections of the ovary in the current study revealed few apoptotic bodies between the granulosa cells. In addition, immunohistochemical stained control sections showed positive immunoreaction for caspase 3 in the nuclei and cytoplasm of a few numbers of granulosa cells, interstitial cells, and luteal cells. In accordance with these findings, Li and Liu^[48] reported that caspase-3 immunoreactivity was relatively abundant in ovarian tissues of control female Sprague-Dawley rats, especially in granulosa cells. Caspase-3 was found in both the nucleus and cytoplasm. Moreover, BCL2 was predominantly cytoplasmic in granulosa cells.

The regulation of apoptosis is primarily carried out by proteins belonging to BCL2 and caspase families. BCL2 is a protein that prevents cell death by stopping mitochondrial liberation of cytochrome c or by combining with factors that activate apoptosis. A proper apoptotic pathway relies on equilibrium between BCL2 and Bax proteins.^[49]

The pro-apoptotic caspase family, which includes caspases 9, 8 and 3, is essential in the process of apoptosis. Caspase-9 is an intrinsic pathway mediator that can be triggered by lack of oxygen and excess ROS. Caspase-8 is vital in the apoptotic pathway triggered by death receptors. Caspase-3 plays a role in cutting crucial cellular proteins, leading to the usual structural apoptosis-related changes observed in cells. Caspase-9 and caspase-8 activation stimulates caspase-3 production, which ultimately results in cell death.^[50]

Numerous apoptotic bodies were detected in granulosa cell layers of secondary and mature follicles of CuO-NPs groups (IB and IIB) of the current study. This increase was also observed in corpora lutea. Statistical analysis of apoptotic bodies and atretic follicles' counts showed that they were significantly increased in group IB and group IIB as compared to group IA and group IIA respectively. Immunohistochemical staining of paraffin sections from these groups for caspase 3 showed a more intense reaction, while immunostaining for BCL2 showed a weak or negative reaction in comparison with control. This was proved statistically. A considerable difference was detected between acute large dose group and chronic small doses group as regard apoptosis parameters (number of apoptotic bodies/HPF and caspase 3 percentage area), indicating that apoptosis was more apparent in the acute CuO-NPs group. According to a prior research conducted by Farshori, et al^[51] for the impact of different doses of nanoparticles of copper oxide on HEp-2 cells, small doses caused changes in cell shape, while increasing the doses caused loss of cellular contents and resulted in cell death after 24 hours exposure.

Moreover, H&E-stained sections from CuO-NPs treated groups (groups IB and IIB) of the current study showed the presence of necrotic debris in Graafian follicles from group IB, and necrotic luteal cells in group IIB. It was reported that the CuO-NPs could trigger apoptosis as well as necrosis to gastric adenocarcinoma cells in a way that varies depending on the dosage. The surface characteristics and reactivity of CuO-NPs were linked to their toxic effects. The small size of nanoparticles enables them to translocate easily across cells, penetrate cell membranes, and induce cell disturbances. Moreover, the spherical shape of CuO-NPs was reported to increase their reactivity.^[8] Nanoparticles have a greater surface area in comparison to larger bulk particles. Increased surface reactivity causes higher generation of ROS and vice versa. Toxicity may also be due to copper ions which are discharged from copper oxide NPs and are harmful to the cells.^[52] Free Cu ions can generate hydroxyl

radicals on the cell's surface, causing cell membrane damage. Copper oxide nanoparticles may be toxic because they build up in lysosomes, where they become more soluble in acidic conditions, releasing highly cytotoxic Cu^{2+} ions into the cytoplasm.^[8] When CuO-NPs were added to incubated human lymphocytes for 24 hours, there was a significant increase in ROS formation.^[53] As ROS generation exceeds the cells' antioxidant capacity, oxidative stress occurs leading to several toxicological outcomes.^[54] In a previous study for the impact of nanoparticles of titanium and zinc on the development, microscopic structure and sustainability of antral follicles, the antral follicles exposed to TiO_2 NPs in culture media showed internalization and agglomeration of the nanoparticles within the cells, causing an increase in follicle size and disruption of the cytoskeleton organization. The presence of trolox, a water-soluble form of vitamin E, helped to partially reduce the effects caused by TiO_2 nanoparticles, suggesting that oxidative stress could have been a factor in mediating these effects. Additionally, ZnO nanoparticles partly dissolved in the culture media, resulting in reduced follicle diameter and disturbed cytoskeletal arrangement, with no protection from Trolox.^[55]

The prominent rise in atretic follicles' count reported in groups treated with CuO-NPs is a remarkable finding in the current study. Follicular atresia is a type of cellular apoptosis. Ovarian tissue damage and cell death in rats injected intraperitoneally with Cu NPs was attributed to hormonal changes, changes in the activity of ovarian genes, activation of apoptosis-triggering factors, and accumulation of ROS.^[56] Increased atretic follicle, inflammation, and necrosis were reported in the ovaries of mice that were administered nano- TiO_2 .

H&E-stained sections from groups IC and IIC (CuO-NPs + selenium treated groups) revealed fewer apoptotic bodies between granulosa cells. Statistical analysis of apoptotic bodies and atretic follicles counts in these groups revealed a significant decrease when compared to copper oxide NPs treated groups. In accordance, immunohistochemical stained sections of these groups for caspase 3 showed less intense positive immunoreaction as compared to CuO-NPs treated groups. These results were confirmed statistically. Selenium was reported to resist apoptosis caused by adverse factors. In addition, it was reported to improve the abnormalities of genes related to apoptosis caused by heavy metal toxicity like lead toxicity.^[57] The anti-apoptotic effect of selenium was attributed to up-regulating BCL2 and down-regulating Bax and cytochrome c.^[58] It was suggested that selenium caused alterations in the mRNA and protein expression within the BCL2/caspase family.^[50] Moreover, in a study of the impact of adding selenium to IVM (In Vitro Maturation) medium on apoptosis in cumulus cells, the results showed a reduction in cells undergoing apoptosis when cumulus-oocyte complexes were matured with selenium. Necrotic cell percentage was reduced in cumulus cells when matured with 100 ng/ml of selenium compared to cumulus cells matured without selenium during IVM. Furthermore, apoptotic cells decreased when 100 ng/ml of selenium were added to the IVM medium.^[59] In another study for the impact of adding selenium on the growth, mortality and proliferation of thyroid follicular cells, the findings suggested that adding selenium enhanced the growth rate of FRTL5 (rat thyroid follicular cell line). In addition, selenium decreased cell death rates by reducing the activity of the proapoptotic genes and increasing the activity of the genes that inhibit apoptosis.^[60]

Selenium, as a crucial component of selenoproteins, is important in both the first and subsequent steps of antioxidant protection. The initial stage stops free radicals' creation. It deactivates catalysts or eliminates free radicals' producing substances and consists of 3 enzymes GPX, SOD, and CAT as well as proteins that bind to metal ions. The initial step is not sufficient to completely stop the production of free radicals within the cell. Consequently, certain radicals evade capture, triggering the peroxidation of lipids and resulting in damage to proteins and DNA. Nevertheless, only GPX4 can interrupt lipid peroxidation, not any other selenoprotein. Therefore, there is a second level of antioxidant protection present. It includes antioxidants that break chains, and additional antioxidants. Thioredoxin is crucial in this second defense mechanism as well. Thioredoxin reductases utilize NADPH to decrease oxidized thioredoxin and its similar proteins, controlling numerous redox signaling events.^[61]

5. Conclusion:

From the present study, copper oxide nanoparticles induced marked histological and immunohistochemical changes in adult rat ovaries at both a single high dose and small repeated doses. Selenium could ameliorate the adverse effects caused by copper oxide nanoparticles, may be through antioxidant and anti-apoptotic mechanisms.

Declaration of Competing Interest

No interesting conflict about this study.

References:

- [1] Ali AS. Application of nanomaterials in environmental improvement. *Environ. Nanotechnol.* 2020;6:17-36.
- [2] SiimKüünal PR, ErwanRauwel. Plant extract mediated synthesis of nanoparticles. In: Barhoum A, Makhlof AS. *Micro and Nano Technologies, Emerging Applications of Nanoparticles and Architecture Nanostructures.* Elsevier, 2018:411-446. Doi: <https://doi.org/10.1016/B978-0-323-51254-1.00014-2>.
- [3] Liu J, DhunganaB, Cobb GP. Environmental behavior, potential phytotoxicity, and accumulation of copper oxide nanoparticles and arsenic in rice plants. *Environ Toxicol Chem.* 2018;37(1):11-20. Doi: <https://doi.org/10.1002/etc.3945>.
- [4] Rex M C, Anand S, Rai PK, Mukherjee A. Engineered Nanoparticles (ENPs) in the Aquatic Environment: an Overview of Their Fate and Transformations. *Water Air Soil Pollut.* 2023;234(7):234-462. Doi: <https://doi.org/10.1007/s11270-023-06488-1>.
- [5] Ighalo JO, Sagboye PA, Umenweke G, Ajala OJ, Omoarukhe FO, Adeyanju CA, et al. CuO nanoparticles (CuO NPs) for water treatment: A review of recent advances. *Environ Nanotechnol Monit Manag.* 2021;15:100443. Doi: <https://doi.org/10.1016/j.enmm.2021.100443>.
- [6] Lead JR, Batley GE, Alvarez PJ, Croteau MN, Handy RD, McLaughlin MJ, et al. Nanomaterials in the environment: behavior, fate, bioavailability, and effects—an updated review. *Environ Toxicol Chem.* 2018;37(8):2029-2063. Doi: <https://doi.org/10.1002/etc.4147>.
- [7] Aloisi M, Rossi G, Colafarina S, Guido M, Cecconi S, Poma AM. The impact of metal nanoparticles on female reproductive system: risks and opportunities. *Int J Environ Res Public Health.* 2022;19(21):13748. Doi: <https://doi.org/10.3390/ijerph192113748>.
- [8] Naz S, Gul A, Zia M. Toxicity of copper oxide nanoparticles: a review study. *IET Nanobiotechnol.* 2020;14(1):1-13. Doi: <https://doi.org/10.1049/iet-nbt.2019.0176>.
- [9] Joshi A, Thiel K, Jog K, Dringen R. Uptake of intact copper oxide nanoparticles causes acute toxicity in cultured glial cells. *Neurochem Res.* 2019;44:2156-2169. Doi: <https://doi.org/10.1007/s11064-019-02855-9>.
- [10] Zaiter T, Cornu R, El Basset W, Martin H, Diab M, Béduneau A. Toxicity assessment of nanoparticles in contact with the skin. *J Nanopart Res.* 2022;24(7):149. Doi: <https://doi.org/10.1007/s11051-022-05523-2>.
- [11] Fahmy HM, Ebrahim NM, Gaber MH. In-vitro evaluation of copper/copper oxide nanoparticles cytotoxicity and genotoxicity in normal and cancer lung cell lines. *J Trace Elem Med Biol.* 2020;60:126481. Doi: <https://doi.org/10.1016/j.jtemb.2020.126481>.
- [12] Al-Musawi MM, Al-Shmgani H, Al-Bairuty GA. Histopathological and biochemical comparative study of copper oxide nanoparticles and copper sulphate toxicity in male albino mice reproductive system. *Int J Biomater.* 2022;2022(1):4877637. Doi: <https://doi.org/10.1155/2022/4877637>.
- [13] Liu H, Lai W, Liu X, Yang H, Fang Y, Tian L, et al. Exposure to copper oxide nanoparticles triggers oxidative stress and endoplasmic reticulum (ER)-stress induced toxicology and apoptosis in male rat liver and BRL-3A cell. *J Hazard Mater.* 2020;401:123349. Doi: <https://doi.org/10.1016/j.jhazmat.2020.123349>.
- [14] Holan V, Javorkova E, Vrbova K, Vecera Z, Mikuska P, Coufalik P, et al. A murine model of the effects of inhaled CuO nanoparticles on cells of innate and adaptive immunity—a kinetic study of a continuous three-month exposure. *Nanotoxicology.* 2019;13(7):952-963. Doi: <https://doi.org/10.1080/17435390.2019.1602679>.

- [15] Thit A, Selck H, Bjerregaard HF. Toxic mechanisms of copper oxide nanoparticles in epithelial kidney cells. *Toxicology in vitro*. 2015;29(5):1053-1059.
- [16] Kieliszek M, Lipinski B, Błażej S. Application of sodium selenite in the prevention and treatment of cancers. *Cells*. 2017;24:6(4):39. doi: 10.3390/cells6040039.
- [17] Akahoshi N, Anan Y, Hashimoto Y, Tokoro N, Mizuno R, Hayashi S, et al. Dietary selenium deficiency or selenomethionine excess drastically alters organ selenium contents without altering the expression of most selenoproteins in mice. *J. Nutr. Biochem*. 2019;69:120-129. Doi: <https://doi.org/10.1016/j.jnutbio.2019.03.020>.
- [18] Qazi IH, Angel C, Yang H, Pan B, Zoidis E, Zeng C-J, et al. Selenium, selenoproteins, and female reproduction: a review. *Molecules*. 2018;23(12):3053. Doi: <https://doi.org/10.3390/molecules23123053>.
- [19] Mojadadi A, Au A, Salah W, Witting P, Ahmad G. Role for selenium in metabolic homeostasis and human reproduction. *Nutrients*. 2021;13(9):3256. Doi: <https://doi.org/10.3390/nu13093256>.
- [20] Amara IB, Troudi A, Garoui E, Hakim A, Boudawara T, Zeghal KM, Zeghal N. Protective effects of selenium on methimazole nephrotoxicity in adult rats and their offspring. *Exp Toxicol Pathol*. 2011;63(6):553-561. Doi: <https://doi.org/10.1016/j.etp.2010.04.007>.
- [21] Karavelioglu E, Boyaci MG, Simsek N, Sonmez MA, Koc R, Karademir M, et al. Selenium protects cerebral cells by cisplatin induced neurotoxicity. *Acta Cir. Bras*. 2015;30(6):394-400. Doi: <https://doi.org/10.1590/S0102-865020150060000004>.
- [22] Bugata LSP, Pitta Venkata P, Gundu AR, Mohammed Fazlur R, Reddy UA, Kumar JM, et al. Acute and subacute oral toxicity of copper oxide nanoparticles in female albino Wistar rats. *J. Appl. Toxicol*. 2019;39(5):702-716. Doi: <https://doi.org/10.1002/jat.3760>.
- [23] Ekambaram G, Kumar SKS, Joseph LD. Comparative study on the estimation of estrous cycle in mice by visual and vaginal lavage method. *J Clin Diagn Res*. 2017;11(1):AC05-AC07. doi: 10.7860/JCDR/2017/23977.9148.
- [24] McLean AC, Valenzuela N, Fai S, Bennett SA. Performing vaginal lavage, crystal violet staining, and vaginal cytological evaluation for mouse estrous cycle staging identification. *J. Vis. Exp*. 2012;(67):e4389. doi: 10.3791/4389.
- [25] Bancroft JD, Layton C. The hematoxylin and eosin. In: Suvarna KS, Layton C, Bancroft JD (eds) *Bancroft's theory and practice of histological techniques. Elsevier health sciences*; 2018; 126-138.
- [26] Kalantari-Hesari A, Morovvati H, Babaei M, Nourian A, Esfandiari K, Elmi T, et al. Modified methods to simplification histochemical, immunohistochemical, and hematoxylin-eosin staining. *Iran J Vet Med*. 2022;18(3):63-73. Doi: 10.22055/IVJ.2022.304383.2398.
- [27] Ghonimi WA, Alferah MA, Dahran N, El-Shetry ES. Hepatic and renal toxicity following the injection of copper oxide nanoparticles (CuO NPs) in mature male Wistar rats: histochemical and Caspase 3 immunohistochemical reactivities. *Environ Sci Pollut Res Int*. 2022;29(54):81923-81937. Doi: <https://doi.org/10.21203/rs.3.rs-1310117/v1>.
- [28] Babu PP, Yoshida Y, Su M, Segura M, Kawamura S, Yasui N. Immunohistochemical expression of BCL2, Bax and cytochrome c following focal cerebral ischemia and effect of hypothermia in rat. *Neurosci. Lett*. 2000;291(3):196-200. Doi: [https://doi.org/10.1016/S0304-3940\(00\)01404-X](https://doi.org/10.1016/S0304-3940(00)01404-X).
- [29] Petrovic A, Abramovic M, Mihailovic D, Gligorijevic J, Zivkovic V, Mojsilovic M, et al. Multicolor counterstaining for immunohistochemistry—a modified Movat's pentachrome. *Biotech Histochem*. 2011;86(6):429-435. Doi: <https://doi.org/10.3109/10520295.2010.528026>.
- [30] Huang KH, Fang WL, Li AFY, Liang PH, Wu CW, Shyr YM, et al. Caspase-3, a key apoptotic protein, as a prognostic marker in gastric cancer after curative surgery. *Int. J. Surg*. 2018;52:258-263. doi: 10.1016/j.ijsu.2018.02.055.
- [31] Dennis PO, Fedoriw Y, Kate EG, Bhargava P. Immunohistology of lymph node and lymph node neoplasms. In: Dabbs DJ (eds) *Diagnostic immunohistochemistry e-book: theranostic and genomic applications. Elsevier Health Sciences*; 2017; 160-202.

- [32] Hazra A, Gogtay N. Biostatistics series module 3: comparing groups: numerical variables. *Indian J Dermatol.* 2016;61(3):251-260.
- [33] Abdelazeim SA, Shehata NI, Aly HF, Shams SGE. Amelioration of oxidative stress-mediated apoptosis in copper oxide nanoparticles-induced liver injury in rats by potent antioxidants. *Sci Rep.* 2020;10(1):10812. Doi: <https://doi.org/10.1038/s41598-020-67784-y>.
- [34] Krishnaiah D, Khiari, M., Klibet, F., Kechrid, Z. Oxidative stress toxicity effect of potential metal nanoparticles on human cells. In: Patel VB., Preedy VR. *Toxicology: Oxidative Stress and Dietary Antioxidants.* Netherlands, Elsevier Science; 2020:107-115.
- [35] Pecoraro BM, Leal DF, Frias-De-Diego A, Browning M, Odle J, Crisci E. The health benefits of selenium in food animals: a review. *J Anim Sci Biotechnol.* 2022; 13(1):1-11. Doi: <https://doi.org/10.1186/s40104-022-00706-2>.
- [36] Yaqub A, Anjum KM, Munir A, Mukhtar H, Khan WA. Evaluation of acute toxicity and effects of sub-acute concentrations of copper oxide nanoparticles (CuO-NPs) on hematology, selected enzymes and histopathology of liver and kidney in *Mus musculus*. *Indian J Anim Res.* 2018;52(1):92-98. Doi: 10.18805/ijar.v0iOF.8489.
- [37] Elkhateeb SA, Ibrahim TR, El-Shal AS, Abdel Hamid OI. Ameliorative role of curcumin on copper oxide nanoparticles-mediated renal toxicity in rats: An investigation of molecular mechanisms. *J Biochem Mol Toxicol.* 2020;34(12):e22593. Doi: <https://doi.org/10.1002/jbt.22593>.
- [38] Ouni S, Askri D, Jeljeli M, Abdelmalek H, Sakly M, Amara S. Toxicity and effects of copper oxide nanoparticles on cognitive performances in rats. *Arch Environ Occup Health.* 2020;75(7):384-394. Doi: <https://doi.org/10.1080/19338244.2019.1689376>.
- [39] Abdel-Halim BR, Moselhy WA, Helmy NA. Developmental competence of bovine oocytes with increasing concentrations of nano-copper and nano-zinc particles during in vitro maturation. *Asian Pac. J. Reprod.* 2018;7(4):161-166. doi: 10.4103/2305-0500.237053.
- [40] Sajjad H, Sajjad A, Haya RT, Khan MM, Zia M. Copper oxide nanoparticles: In vitro and in vivo toxicity, mechanisms of action and factors influencing their toxicology. *Comp Biochem Physiol C Toxicol Pharmacol.* 2023;271:109682. Doi: <https://doi.org/10.1016/j.cbpc.2023.109682>.
- [41] Huang C, Wu D, Khan FA, Wang Y, Xu J, Luo C, et al. Zinc oxide nanoparticle causes toxicity to the development of mouse oocyte and early embryo. *Toxicol Lett.* 2022;358:48-58. Doi: <https://doi.org/10.1016/j.toxlet.2022.01.010>.
- [42] Zhao J, Dong L, Lin Z, Sui X, Wang Y, Li L, Liu T, Liu J. Effects of selenium supplementation on polycystic ovarian syndrome: a systematic review and meta-analysis on randomized clinical trials. *BMC Endocr. Disord.* 2023;23(1):33. Doi: <https://doi.org/10.1186/s12902-023-01286-6>.
- [43] Xiong X, Lan D, Li J, Lin Y, Li M. Selenium supplementation during in vitro maturation enhances meiosis and developmental capacity of yak oocytes. *Anim Sci J.* 2018;89(2):298-306. Doi: <https://doi.org/10.1111/asj.12894>.
- [44] Kaur S, Saluja M, Aniq A, Sadwal S. Selenium attenuates bisphenol A incurred damage and apoptosis in mice testes by regulating mitogen-activated protein kinase signalling. *Andrologia.* 2021;53(3):e13975. Doi: <https://doi.org/10.1111/and.13975>.
- [45] Amelkina O, Braun BC, Dehnhard M, Jewgenow K. The corpus luteum of the domestic cat: histologic classification and intraluteal hormone profile. *Theriogenology.* 2015;83(4), 711-720. Doi: <https://doi.org/10.1016/j.theriogenology.2014.11.008>.
- [46] Fatahian-Dehkordi RA, Reaisi M, Heidarnejad MS, Mohebbi A. Serum biochemical status and morphological changes in mice ovary associated with copper oxide nanoparticles after thiamine therapy. *J. Herbm Pharmol.* 2016;6(1), 21-26.
- [47] Taketa Y. Luteal toxicity evaluation in rats. *J. Toxicol. Pathol.* 2022;35(1):7-17. Doi: <https://doi.org/10.1293/tox.2021-0058>.
- [48] Li N, Liu L. Mechanism of resveratrol in improving ovarian function in a rat model of premature ovarian insufficiency. *J Obstet Gynaecol Res.* 2018;44(8):1431-1438. Doi: <https://doi.org/10.1111/jog.13680>.

- [49] Marinova M. Effects of NAD⁺ booster NMN on ovarian function and late-life bone health. Doctoral dissertation, UNSW Sydney, 2022;1-17. <http://hdl.handle.net/1959.4/100825>.
- [50] Gao J, Tian X, Yan X, Wang Y, Wei J, Wang X, Yan X, Song G. Selenium exerts protective effects against fluoride-induced apoptosis and oxidative stress and altered the expression of BCL2/Caspase family. *Biol. Trace Elem. Res.* 2021;199:682-692. Doi: <https://doi.org/10.1007/s12011-020-02185-w>.
- [51] Farshori NN, Siddiqui MA, Al-Oqail MM, Al-Sheddi ES, Al-Massarani SM, Ahamed M, et al. Copper oxide nanoparticles exhibit cell death through oxidative stress responses in human airway epithelial cells: a mechanistic study. *Biol. Trace Elem. Res.* 2022;200(12):5042-5051. Doi: <https://doi.org/10.1007/s12011-022-03107-8>.
- [52] Gopinath V, Priyadarshini S, Al-Maleki A, Alagiri M, Yahya R, Saravanan S, et al. In vitro toxicity, apoptosis and antimicrobial effects of phyto-mediated copper oxide nanoparticles. *RSC Adv.* 2016;6(112):110986-110995. Doi: 10.1039/C6RA13871C.
- [53] Assadian E, Zarei MH, Gilani AG, Farshin M, DegampanahH, Pourahmad J. Toxicity of copper oxide (CuO) nanoparticles on human blood lymphocytes. *Biol. Trace Elem. Res.* 2018;184:350-357. Doi: <https://doi.org/10.1007/s12011-017-1170-4>.
- [54] Mannucci A, Argento FR, Fini E, Coccia ME, Taddei N, Becatti M, et al. The impact of oxidative stress in male infertility. *Front. mol. biosci.* 2022;8:799294. Doi: <https://doi.org/10.3389/fmolb.2021.799294>.
- [55] Santacruz-Márquez R, Solorio-Rodríguez A, González-Posos S, García-Zepeda SP, Santoyo-Salazar J, De Vizcaya-Ruiz A, et al. Comparative effects of TiO₂ and ZnO nanoparticles on growth and ultrastructure of ovarian antral follicles. *ReprodToxicol.* 2020;96:399-412. Doi: <https://doi.org/10.1016/j.reprotox.2020.08.003>.
- [56] Yang J, Hu S, Rao M, Hu L, Lei H, Wu Y, et al. Copper nanoparticle-induced ovarian injury, follicular atresia, apoptosis, and gene expression alterations in female rats. *Int. J. Nanomed.* 2017;5959-5971. Doi: <https://doi.org/10.2147/IJN.S139215>.
- [57] Hong W, Liu Y, Liang J, Jiang C, Yu M, Sun W, et al. Molecular Mechanisms of Selenium Mitigating Lead Toxicity in Chickens via Mitochondrial Pathway: Selenoproteins, Oxidative Stress, HSPs, and Apoptosis. *Toxics.* 2023;11(9):734. Doi: <https://doi.org/10.3390/toxics11090734>.
- [58] Fang Y, Xu Z, Shi Y, Pei F, Yang W, Ma N, et al. Protection mechanism of Se-containing protein hydrolysates from Se-enriched rice on Pb²⁺-induced apoptosis in PC12 and RAW264.7 cells. *Food Chem.* 2017;219:391-398. Doi: <https://doi.org/10.1016/j.foodchem.2016.09.131>.
- [59] Lizarraga RM, Anchordoquy JM, Galarza EM, Farnetano NA, Carranza-Martin A, Furnus CC, Mattioli GA, Anchordoquy JP. Sodium selenite improves in vitro maturation of bosprimigeniustaurus oocytes. *Biol. Trace Elem. Res.* 2020;197:149-158. Doi: <https://doi.org/10.1007/s12011-019-01966-2>.
- [60] Nettore IC, De Nisco E, Desiderio S, Passaro C, Maione L, Negri M, et al. Selenium supplementation modulates apoptotic processes in thyroid follicular cells. *BioFactors.* 2017;43(3):415-423. Doi: <https://doi.org/10.1002/biof.1351>.
- [61] Zoidis E, Seremelis I, KontopoulosN, Danezis GP. Selenium-dependent antioxidant enzymes: Actions and properties of selenoproteins. *Antioxidants.* 2018;7(5):66. Doi: <https://doi.org/10.3390/antiox7050066>.

